Kovove Mater. 61 2023 35–48
DOI: 10.31577/km.2023.1.35

Compressive properties of an Al-matrix syntactic foam filled with Al_2O_3 hollow sphere

Haobo Qu[1], Chao Yang[1], Junge Cui[1], Danlin Huang[2], Zheyang Lin[1], Huabing Lu[1], Liwen Pan[1]*

[1] *Guangxi Key Laboratory of Processing for Non-Ferrous Metal and Featured Materials, School of Resources, Environment and Materials, Guangxi University, Nanning 530004, P. R. China*
[2] *Dean's Office of Guangxi University, Nanning 530004, P. R. China*

Received 12 October 2022, received in revised form 5 November 2022, accepted 14 November 2022

Abstract

Al_2O_3 hollow spheres were implanted in cast Al-Si-Cu-Mg alloy to prepare Al-matrix syntactic foams by gravity infiltration casting. The effects of hollow sphere size and heat treatment on microstructure, quasi-static compressive properties, and energy absorption properties of the Al-matrix syntactic foams were investigated. The results show that hollow sphere size is the most critical factor affecting the compressive and energy absorption properties. The plateau strength and specific energy absorption of the syntactic foam increase with the decrease of the hollow sphere size. The as-cast syntactic foams with a sphere size of 0.5–1 mm have the highest plateau strength and specific energy absorption, reaching 66.55 MPa and 20.38 kJ kg^{-1}, respectively. The compressive properties of all heat-treated syntactic foams are significantly improved compared with the as-cast. The maximum plateau strength and specific energy absorption are 87.71 MPa and 30.45 kJ m^{-3}, respectively. The fundamental reason why small hollow spheres are more conducive to improving compression performance is that small spheres in the syntactic foam are subject to less leverage torque and are not accessible to damage; they can withstand more significant compressive stress. The improvement of the compressive properties of the heat-treated syntactic foam is mainly attributed to the release of residual compressive stress.

K e y w o r d s: Al-matrix syntactic foam, hollow sphere size, heat treatment process, compression performance, energy absorption ability

1. Introduction

Metal matrix syntactic foams (MMSFs) are a new structural and functional porous material that scientists have been widely attracted in the recent twenty years. The appeal of MMSFs includes lightweight, high specific compressive strength, high energy absorption capacity, high fatigue strength, high thermal insulation, and low thermal expansion coefficient [1–9]. High energy absorption capacity is the main advantage compared to metal foams prepared by the traditional foaming method [2, 10–14]. Superior performances of MMSFs benefit from the core-shell structure of the filled hollow spheres [15]. The core-shell structure and high-volume fraction of spheres make the syntactic foam have high compressive stress and long plateau strain suitable for energy absorption application. High energy absorption properties provide MMSFs with great potential for applications in energy absorbers, sound absorbers, collision dampers, blast protection, and ballistic armours of aircraft, spacecraft, vehicles, and ship fields [1, 16].

Aluminium alloys are the most used matrix materials for metal syntactic foams due to their lightweight, high specific strength, and low cost. Different matrix materials of aluminium alloy matrix syntactic foams have been researched a lot in recent years, such as A6061 [17], 5A03 [2, 4], 5A06 [4], A380 [18], and A356 [15, 19–26], in which cast aluminium alloys containing silicon were used mainly due to their excellent mechanical properties and casting behaviour. At present, the preparation method of aluminium matrix syntactic foams includes pressure infiltration casting [1, 2, 4, 18, 27, 28], squeeze casting, stir casting [17], grav-

*Corresponding author: e-mail address: panliwen@gxu.edu.cn

Table 1. Basic parameters of alumina hollow spheres

Chemical composition (%)				Bulk density ($g\,cm^{-3}$)	Particle size (mm)	Application temperature (℃)
Al_2O_3	Fe_2O_3	SiO_2	Na_2O			
> 99	0.15 ± 0.05	0.2 ± 0.1	0.25 ± 0.05	0.5–1	0.2–5	1800

ity infiltration casting [3, 19, 20, 29, 30], and vacuum dies casting [10]. Powder metallurgy [31, 32], in which gravity infiltration casting is the simplest and of the lowest cost, is more suitable for industrial production. However, only the static pressure of liquid metal is often not enough, especially when the gap between the hollow spheres is tiny (such as micron-scale hollow spheres). Therefore, large hollow particles (millimetre-sized) are often used in gravity infiltration casting [20, 21, 30].

In addition to the matrix alloy and the preparation method, the type and size of hollow spheres and the subsequent heat treatment all affect the compressive properties of aluminium matrix syntactic foam. A. Kemény's research [33] showed that the Al-matrix syntactic foam filled with ceramic hollow spheres is suitable for use as high-performance and lightweight structural components. The syntactic foam filled with the hollow metal sphere is suitable for energy absorption applications (such as protective devices and collision dampers). The syntactic foam filled with lightweight expanded clay particles is suitable for large quantities of low-cost and high-energy absorption applications. Alexandra Kemény's research [29, 34] showed that the compression curves of Al-matrix syntactic foam jointly filled with large and small ceramic hollow spheres show a double-peak characteristic, and the proportion of both can be adjusted to adapt to different application fields. H. Puga [30] researched the effect of expanded clay particle diameter on the mechanical properties of Al-matrix syntactic foams, which showed that the syntactic foams filled with smaller particles have a higher density while getting lower densification strain and compressive yield strength. The research of T. Fiedler [20] showed that greater expanded glass particle size increases the grain size of the matrix of the final Al-matrix syntactic foams. In contrast, smaller particles decrease plateau strength oscillation and enhance the energy absorption properties of the resulting Al-matrix syntactic foams. H. Puga [35] investigated Al-matrix syntactic foams filled with different diameters of lightweight expanded clay prepared by gravity casting, which indicated diameters play a predominant role in the density and compressive properties of the syntactic foams. Smaller particles generate higher densities while reducing strain densification. Additionally, a higher particle diameter generates higher yield strength and a more constant stress value during the plateau region, which gains higher crushing energy absorption. M. Taherishargh [19] investigated A356 Al-matrix syntactic foams filled with different size ranges of expanded perlite particles prepared by molten infiltration, which indicated decreasing the hollow particle size resulting in improving plateau strength and energy absorption capacity. However, these references do not clearly explain the effect of hollow particle size on syntactic foam compression performance. In addition, heat treatment also has a significant effect on the compressive properties of metal syntactic foams [36, 37], mainly due to the change of matrix microstructure and the elimination of residual stress.

It is worth mentioning that there are few kinds of literature to comprehensively study the effect of the size of hollow spheres and heat treatment technology on the compression performance of aluminium matrix syntactic foams made by gravity infiltration casting. In this paper, different size ranges of Al_2O_3 hollow spheres were filled in a cast Al-Si-Cu-Mg alloy to prepare Al-matrix syntactic foams. The combined influence of hollow sphere size and heat treatment process on microstructure and compressive properties of Al-matrix syntactic foam were discussed.

2. Methodology

2.1. Materials

Al_2O_3 hollow spheres were provided by Gongyi City Hongle Mineral Products Co., Ltd (P. R. China). According to the product data sheet provided by the manufacturer, some parameters of Al_2O_3 hollow spheres are shown in Table 1. The griddle screened the particle size ranges of 0.5–1 mm, 1–2 mm, and 2–3 mm. The hollow spheres with broken core-shell were removed from the water by the gravity sedimentation method. The intact Al_2O_3 hollow spheres taken from water were cleaned in an alcoholic solution for 5 min by the ultrasonic cleaner and then were dried at 200 ℃ for 3 h. The matrix alloy is cast Al-Si-Cu-Mg alloy, and the chemical composition is shown in Table 2. High Si content gives the matrix alloy good castability. Adding Cu and Mg increases the mechanical properties of the matrix due to the presence of the Al_2Cu precipitated phase. Moreover, the presence of Mg also improves the wettability between the aluminium melt and the hollow spheres [38].

Table 2. Chemical composition of cast Al-Si-Cu-Mg matrix alloy (wt.%)

Si	Cu	Mg	Ti	Mn	Al
12.5 ± 0.3	2.5 ± 0.2	1.2 ± 0.1	0.3 ± 0.1	0.2 ± 0.1	remain

Table 3. Heat treatment processes applied to AMSFs

Type of heat treatment	Temperature (℃)	Time (h)	Cooling method	Temperature (℃)	Time (h)	Cooling method
Homogenization	515	1	Air cooling	–	–	–
Homogenization	515	2	Air cooling	–	–	–
Homogenization-ageing	515	1	Air cooling	165	3	Air cooling
Homogenization-ageing	515	1	Air cooling	165	5	Air cooling

2.2. Matrix alloy smelting

The matrix alloys were smelted in a medium-frequency induction furnace using a graphite crucible coated with a mixture of zinc oxide and sodium silicate. Firstly, some piece of pure aluminium (99.9 wt.%) was independently put into the graphite crucible and heated. When the aluminium block was completely melted, a thermocouple was inserted into the melt to measure the melt temperature. The heating power was adjusted to keep the melt temperature at about 760 ℃ for 3–4 min. After that, instantly soluble silicon (95 wt.% Si) was added to the melt and held for 7–8 min at 760 ℃ after adding the covering agent. After slagging off, the master alloys Al-50Cu, Al-10Mn, Al-10Ti, and purity magnesium sheet were intermittently and orderly added to the melt. This process lasts about 5–6 min. In the meantime, the melt temperature was gradually cooled to about 720 ℃. Finally, the melt was degassed by adding hexachloroethane and poured into a steel mould with a diameter of 18 mm and a height of 160 mm after slagging off again. The casting rod was cut into the dimension ø 18 × 150 mm^2 used for the gravity infiltration test.

2.3. Gravity infiltration casting

In this experiment, Al-matrix syntactic foam was prepared by gravity infiltration casting technology that our research group had used before [39]. Firstly, different particle sizes of alumina hollow spheres with a volume of about 25 cm^3 were put into a corundum tube (inner diameter 20 mm, height 250 mm. The tube was shaken manually to make the hollow spheres compact. Then, the ceramic tube was vertically placed into a resistance furnace and heated. The furnace temperature was held at 500 ℃ for 1 h, and then the prepared Al-Si-Cu-Mg alloy cast rod was placed into the ceramic tube and continued to heat up. When the cast rod was melted entirely, a certain amount of covering agent (NaCl : KCl = 1 : 1; (wt.%)) was added into the melt to prevent volatilization. Finally, the infiltration temperature (the melt temperature) was set at 750 ℃, and the infiltration time was 60 min. After the infiltration, the ceramic tube was taken out for cooling in the air.

2.4. Heat treatment process and microstructure observation

The effect of heat treatment on the compressive properties of metal matrix syntactic foams currently lacks systematic research. Therefore, most heat treatment processes applied to syntactic foams were based on strengthening and toughening matrix alloys and eliminating and releasing the residual stress. Combined with previous studies [2, 40–43], we found that homogenization and ageing played an essential role in the compressive properties of metal syntactic foams, so the homogenization and ageing process (as shown in Table 3) were applied to Al-matrix syntactic foams in this study. Heat treatment experiments were carried out in a tubular resistance furnace (model SK2-4--12). The microstructure of the matrix and interface of the syntactic foams for as-cast and heat-treated samples were observed by Phenom ProX scanning electron microscope (SEM), and the built-in energy dispersive spectroscopy (EDS) was used for component analysis.

2.5. Quasi-static compression testing

This study used cuboid specimens for a quasi-static compression test, and the dimension was 10 × 10 × 15 mm^3. The processed specimens are shown in Fig. 1. Uniaxial compression test for Al-matrix syntactic foams was conducted on a universal testing machine (WDW3100) in the atmosphere. The compression strain rate is constant at $10^{-3}\,s^{-1}$. During the experiment, testing machine system software recorded loading and displacement data, which generated the

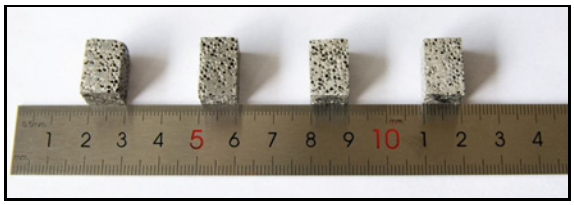

Fig. 1. Macrograph of Al-matrix syntactic foam compressive test samples.

engineering stress-strain curves from which the material properties were calculated.

2.6. Evaluation criteria for energy absorption performance

In general, the compressive energy absorption property index of MMSFs mainly included compressive strength (σ_{bc}), average plateau stress ($\bar{\sigma}$), densification strain (ε_D), energy absorption capacity (W), specific energy absorption (E_s), and energy absorption efficiency (ξ).

ε_D is the strain value when the hollow spheres in the MMSFs are just fully compacted, defined as densification strain [44]. The tangent method is used to determine the ε_D value [45, 46].

Plateau strength ($\bar{\sigma}$) is the average stress on the stress platform; the formula is:

$$\bar{\sigma} = \sum_{n\varepsilon_A}^{n\varepsilon_D} \sigma_i / n, \tag{1}$$

where ε_A and ε_D refer to the starting point and ending point of the stress platform, respectively.

The energy absorbed per unit volume is called energy absorption capacity. Through calculation under compression stress-strain curve until the densification strain epsilon (ε_D) area to determine the energy absorption capacity, the formula can be expressed as follows [2, 44]:

$$W = \int_0^{\varepsilon_D} \sigma(\varepsilon) \mathrm{d}\varepsilon. \tag{2}$$

Specific energy absorption (E_s) describes materials' impact resistance. It can be used to evaluate the absorbed energy under the same mass, and its formula is as follows [15, 44]:

$$E_s = \frac{W_{\varepsilon_D}}{\rho_0}, \tag{3}$$

where W_{ε_D} is the energy absorption capacity of the material and ρ_0 is the density of Al-matrix syntactic foams.

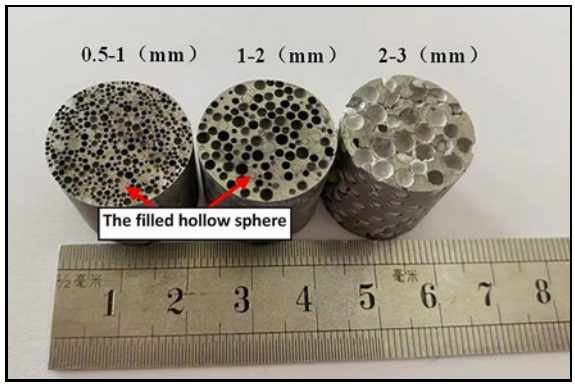

Fig. 2. Macrograph of Al-matrix syntactic foam filled with hollow spheres of different diameters.

Energy absorption efficiency (ξ) is the ratio between the energy absorbed by the material in the actual compression process and the energy absorbed by the ideal compression process under any strain. The calculation formula [19, 44] is as follows:

$$\xi = \frac{A_{real}}{A_{ideal}} = \frac{\int_0^{\varepsilon_D} \sigma(\varepsilon) \mathrm{d}\varepsilon}{\sigma_{max}\varepsilon_D}, \tag{4}$$

where A_{real} is the actual energy absorption, A_{ideal} is the ideal energy absorption, σ_{max} is the compressive stress, and maximum stress at a point ε_D.

3. Results and discussion

3.1. Structure of the syntactic foam

The macrograph of Al-matrix syntactic foam filled with different sizes of hollow spheres is shown in Fig. 2. It can be seen that the gaps between hollow spheres are filled with aluminium alloy melt, while the syntactic foam is filled with small hollow spheres or large ones. It can be seen from the cross-section that the distribution of hollow microspheres in the aluminium matrix is relatively uniform, and most of the hollow microspheres are intact; only a tiny amount is filled with aluminium liquid, as shown by the red arrow in the figure. We believe that a small number of hollow spheres filled by the matrix indicate the shell is fragile or has congenital disabilities, and the shell cracks during the infiltration process, causing the metal liquid to fill in.

Figure 3 shows the as-cast microstructure of syntactic foam filled with hollow spheres with different particle sizes. According to the EDS composition analysis in Fig. 4 and some references, the syntactic foams are composed of Al_2O_3, α-Al, Al_2Cu, Si phase, Q phase (Al-Si-Mg-Cu) [47], $(Si, Al)_3Ti$. The hollow sphere shell is composed of the Al_2O_3 phase,

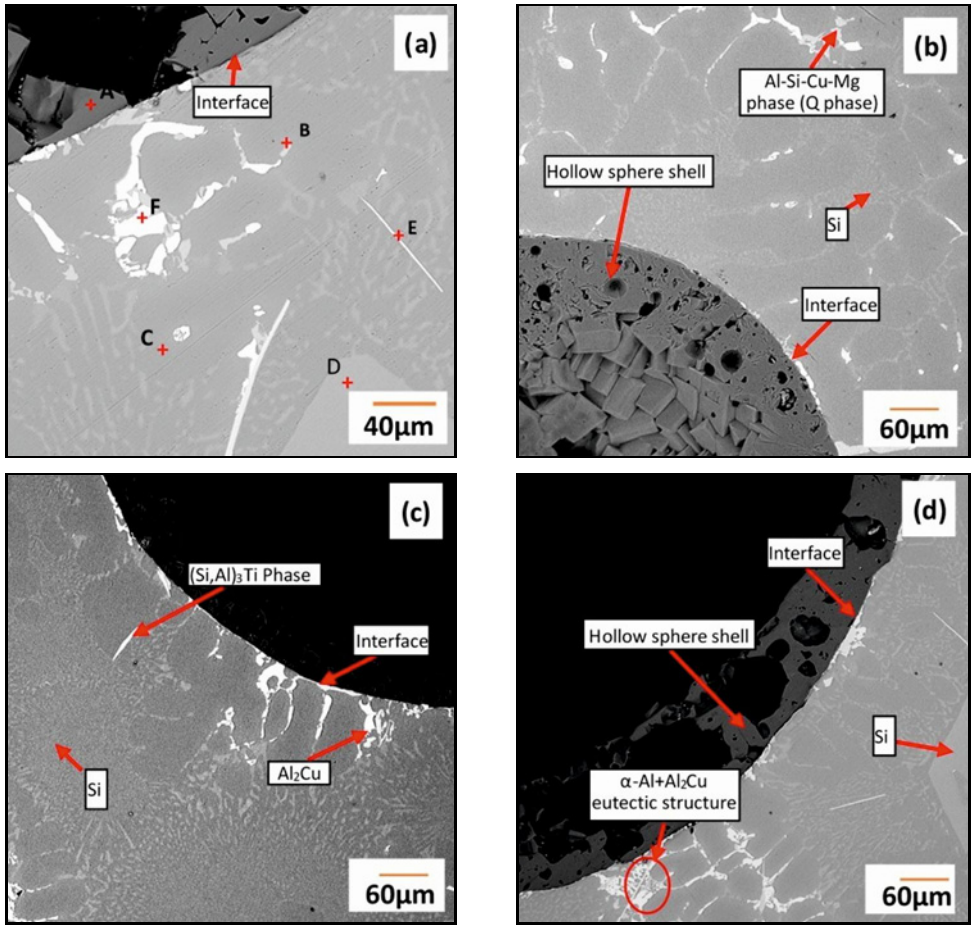

Fig. 3. Microstructure of the as-cast syntactic foams filled with hollow spheres of different sizes; (a) EDS point analysis positions (1–2 mm), (b) 0.5–1 mm, (c) 1–2 mm, and (d) 2–3 mm.

as shown by the red arrow in Fig. 3. Al_2Cu phase is white granular or skeleton, as shown by the red arrow in Fig. 3. Some Al_2Cu phases are of the network skeleton structure and α-Al forms eutectic structure. A small amount of the grey-white Q phase is symbiotic with the Al_2Cu phase. Almost all Si and α-Al are distributed around the matrix grains in the eutectic state, and Si is in a granular or blocky state. In addition, the matrix has a long white strip $(Si, Al)_3Ti$ phase [48]. It can be seen from Fig. 3 that the interface of the syntactic foam filled with different hollow spheres is relatively straightforward, dense, and continuous, and there is no gap, indicating that the interface is tightly bonded. We believe that adding Mg to the melt helps to improve the wettability [49].

3.2. Heat treatment microstructure of the syntactic foam

Figure 5 shows the microstructure photo of the syntactic foams with a hollow sphere size of 0.5–1 mm after heat treatment. It can be seen that the microstructure of the syntactic foam matrix after homogenization for 1 and 2 h has changed compared with the as-cast syntactic foam (Fig. 3a), mainly due to the coarsening of Si particles. The Si particles normalized for 2 h are coarser than those normalized for 1 h. It shows that the Si phase is unstable and easy to coarsen at the homogenization temperature (515 ℃). After homogenization, the Q phase and $(Si, Al)_3Ti$ almost disappear, while the size and morphology of the Al_2Cu phase almost remain unchanged. After homogenization and ageing treatment, the most significant change in the microstructure of the syntactic foam is that the Si particles have agglomerated and coarsened. The longer the ageing time is, the larger the Si phase is. Other phases have little change.

3.3. Density and porosity

The density of the matrix alloy and syntactic foam is calculated by measuring the mass and volume of the samples. The calculation formula is:

$$\rho = m/v, \tag{5}$$

where m is the mass of composite foam and v is the volume of composite foam.

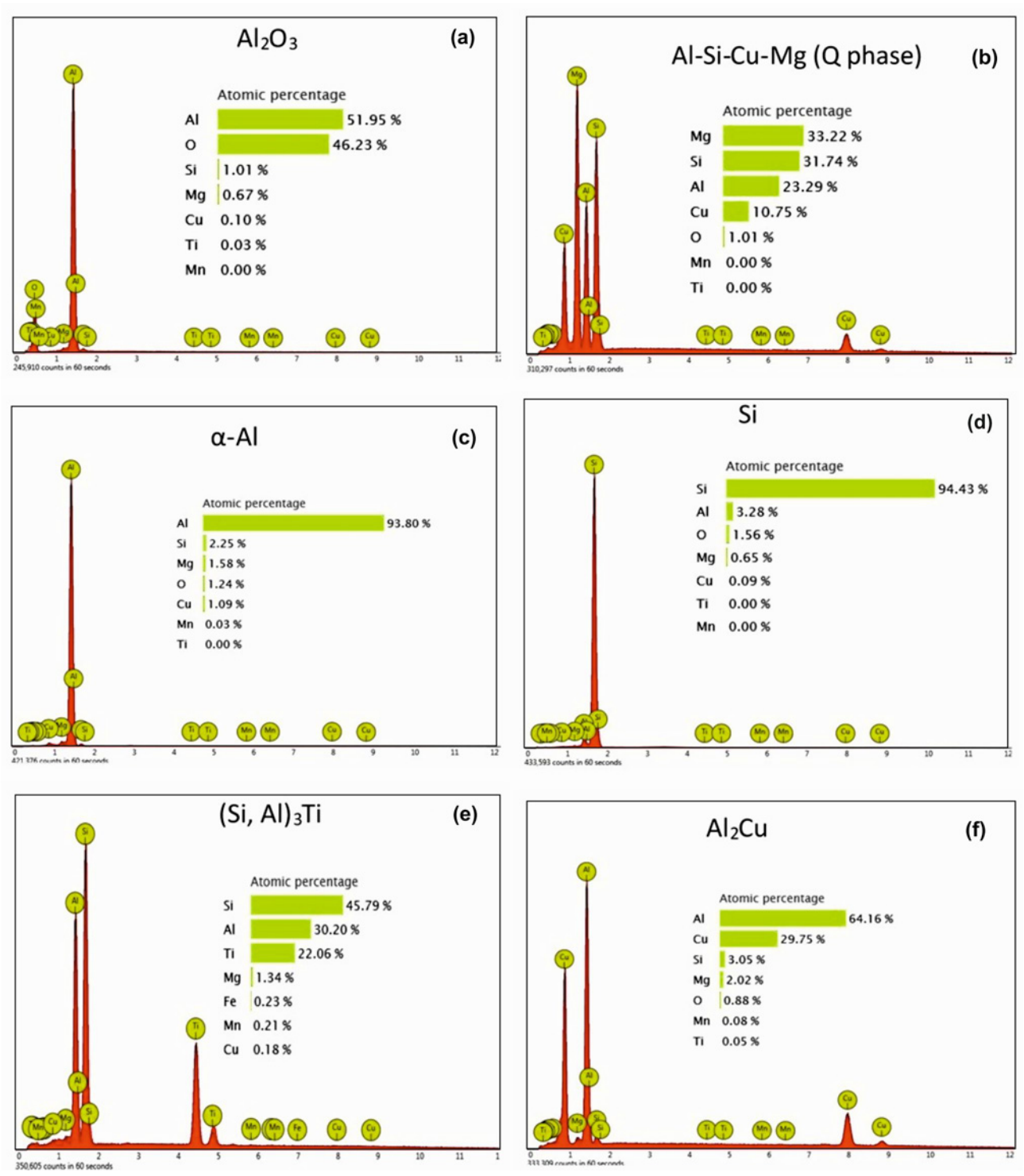

Fig. 4. EDS composition analysis of each point in Fig. 3a.

The porosity is approximately calculated by the relative density of the syntactic foam and matrix alloy, and the formula [50] is as follows:

$$P = 1 - \rho_{\mathrm{sf}}/\rho_{\mathrm{m}}, \tag{6}$$

where P is the porosity of the syntactic foam, ρ_{sf} and ρ_{m} represent the density of the syntactic foam and matrix alloy, respectively.

It can be seen from Table 4 that the density and porosity of syntactic foams prepared with different hollow sphere sizes are quite different. With the particle size increase, the density of syntactic foam decreases while the porosity increases. The syntactic

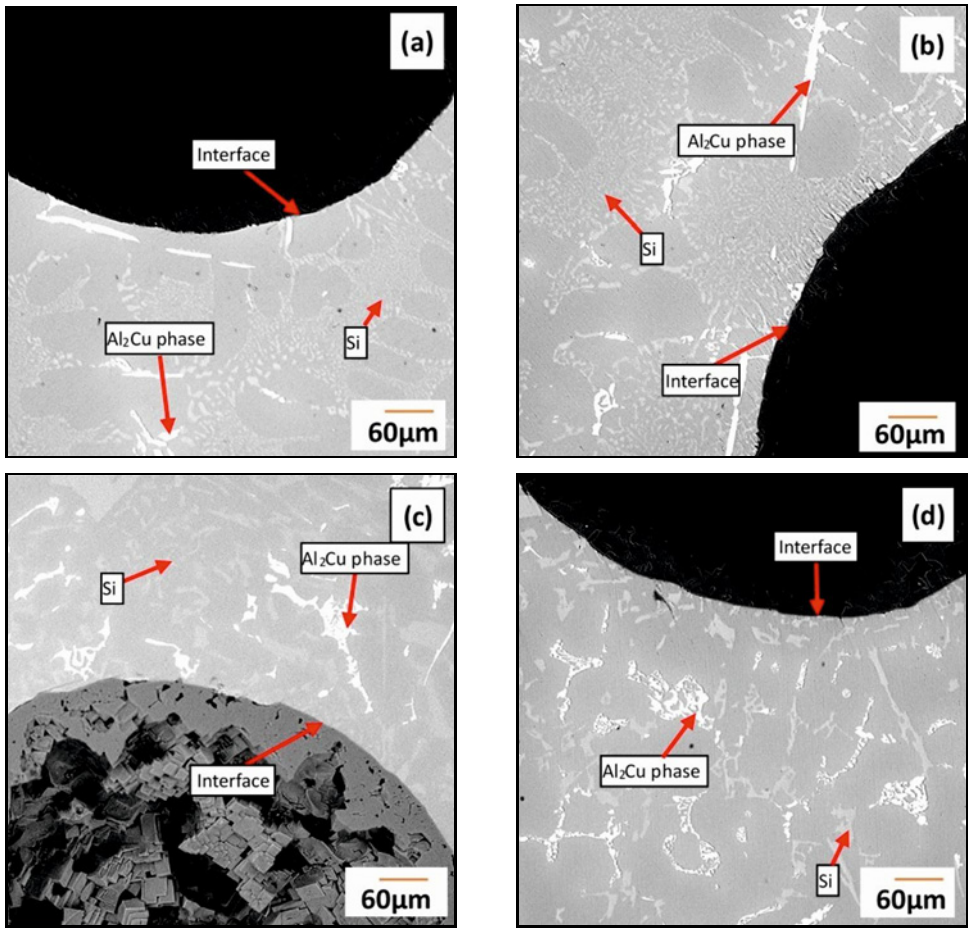

Fig. 5. Microstructure of the syntactic foams after heat treatment: (a) 515 °C/1 h/AC, (b) 515 °C/2 h/AC, (c) 515 °C/1 h/AC + 165 °C/3 h/AC, and (d) 515 °C/1 h/AC + 165 °C/5 h/AC.

Table 4. Density and porosity in syntactic foams

Factors	Parameter	Density (g cm^{-3})	Porosity (%)
Hollow sphere size (mm)	0.5–1	1.82 ± 0.03	35.80 ± 1.58
	1–2	1.67 ± 0.02	41.04 ± 0.42
	2–3	1.61 ± 0.04	42.75 ± 0.71
Heat treatment process	515 °C/1 h/AC	1.82 ± 0.02	35.77 ± 1.53
	515 °C/2 h/AC	1.83 ± 0.02	34.65 ± 0.88
	515 °C/1 h/AC + 165 °C/3 h/AC	1.75 ± 0.08	37.33 ± 2.74
	515 °C/1 h/AC + 165 °C/5 h/AC	1.73 ± 0.05	38.50 ± 2.17
Average		1.75	37.98

foam with an average particle size of 2–3 mm has the highest porosity, reaching 42.75 %. After heat treatment, the density of composite foam prepared from hollow microspheres with the same particle size range changes slightly. The change in the matrix microstructure should cause it. On the whole, the overall porosity changes little. The average density of all syntactic foam samples is 1.75 g cm^{-3}, and the average porosity is 37.98 %.

3.4. Compressive property and energy absorption property

The compression stress-strain curves of the as-cast syntactic foam filled with different sizes of hollow spheres are shown in Fig. 6a. Figure 6b shows the compression stress-strain curves of the syntactic foam after heat treatment. Table 6 shows Al-matrix syntactic foam's compression and energy absorption

Table 5. Compressive properties and energy absorption properties of Al-matrix syntactic foams

Factors	Parameters	Compressive strength (MPa)	Plateau strength (MPa)	Densification strain (%)	Energy capacity absorption (MJ m^{-3})	Specific absorption energy (kJ kg^{-1})	Energy efficiency absorption (%)
Particle size (mm)	0.5–1	88.0	66.55	52.76	37.10	20.38	81.23
	1–2	60.5	53.46	62.31	32.42	19.53	80.85
	2–3	48.8	27.25	37.69	10.71	6.61	80.17
Heat treatment	515 ℃/1 h/AC	120.2	87.71	61.48	56.33	30.45	81.24
	515 ℃/2 h/AC	106.2	87.10	63.91	54.25	29.48	89.40
	515 ℃/1 h/AC + 165 ℃/3 h/AC	117.3	76.47	55.81	47.31	27.51	85.27
	515 ℃/1 h/AC + 165 ℃/5 h/AC	93.0	75.17	58.87	45.46	27.06	87.39

Table 6. The particle size range, average particle size, average wall thickness of Al_2O_3 hollow spheres

Particle size range (mm)	Mean diameter, D (μm)	Mean wall thickness, t(μm)	Mean wall thickness to diameter ratio, t/D	Mean wall thickness to radius ratio, t/R
0.5–1	850	41.3	0.049	0.097
1–2	1480	70.1	0.047	0.095
2–3	2580	117.0	0.045	0.091

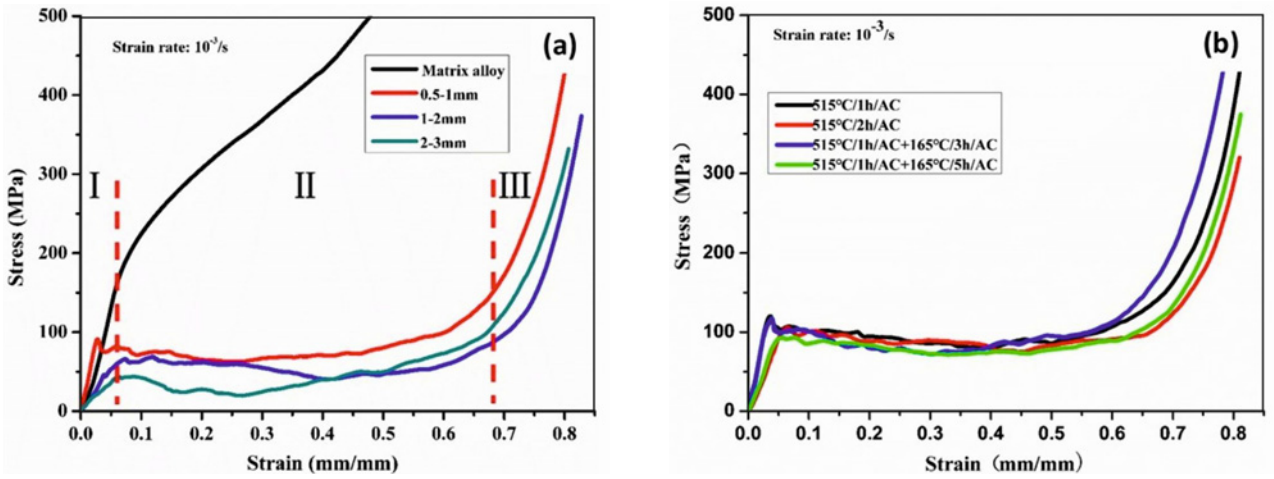

Fig. 6. Compressive stress-strain curves of the Al-matrix syntactic foams: (a) as-cast syntactic foams with different hollow sphere sizes and (b) heat-treated syntactic foams.

performance data. It can be seen from Fig. 6a that the compression curve of the matrix alloy almost rises sharply with the increase of strain (strain hardening process). The compression curve of syntactic foam filled with hollow spheres with different particle sizes can be roughly divided into three stages, namely the linear elastic stage (I), platform stage (II), and densification stage (III). The syntactic foam's compression curve conforms to the metal foam's compression characteristics [15, 32, 40, 51–53]. The strain range of the plateau area is about 0.05–0.7. It can be seen that the compressive strength and plateau height of the syntactic foam show a significant downward trend with the increase of the hollow sphere size. The compressive strength and plateau height of the syntactic foam with 0.5–1 mm hollow spheres are the highest, reaching 88–66.55 MPa, respectively. The compressive strength and plateau height of the syntactic foam with hollow spheres of 2–3 mm are the lowest, only 48.8 and 27.25 MPa, respectively. In addition, from the shape of the compression curve, it can be seen that the smaller the hollow spheres are, the more even the compression plateau area is. The plateau of the syntactic foam with large hollow spheres fluctuates rapidly, which is not conducive to the energy absorption and vibration reduction process. It can also be seen from Table 6 that

the energy absorption capacity, specific energy absorption, and energy absorption efficiency of aluminium matrix syntactic foam are inversely proportional to the particle size of the filled hollow spheres. The syntactic foam with a hollow sphere size of 2–3 mm has lower energy absorption capacity and specific energy, 10.71 MJ m^{-3} and 6.61 kJ kg^{-1}, respectively. The absorption capacity and specific energy absorption of the syntactic foam with the hollow sphere size of 0.5–1 mm are the highest, reaching 37.10 MJ m^{-3} and 20.38 kJ kg^{-1}, respectively.

It can be seen from Fig. 3 that there is no significant difference in the phase types, size, shape, quantity, and distribution of the as-cast syntactic foams filled with different sizes of Al_2O_3 hollow spheres, while the compression performance of syntactic foam prepared with different hollow sphere sizes is quite different. We believe that hollow spheres' particle size mainly determines syntactic foam's compression performance. In order to more precisely describe the impact of hollow sphere size on the compression performance, we conducted statistical analysis on Al_2O_3 hollow spheres with different particle size ranges. The particle size range, average particle size, average wall thickness, and the ratio of average wall thickness to average diameter (t/D) are shown in Table 6. It can be seen that the ratio of wall thickness to diameter (t/D) decreases with the increase of hollow sphere size, which is consistent with the decrease of syntactic foam compression performance with the increase of hollow particle size, that is, t/D value is proportional to the compression strength. According to the mixing rule of composite materials, the strength of composite materials is mainly determined by the strength of reinforcement when the strength of the matrix is unchanged. In this experiment, the matrix materials are the same, so the compressive strength of the syntactic foam change is mainly caused by the difference in the strength or stress of the hollow spheres. When the hollow sphere diameter D is constant, the t/D value increases with the wall thickness t. The greater the wall thickness t, the greater the strength of the hollow sphere due to the same hollow sphere material; the larger the t/D value, the greater the compression strength of the syntactic foam.

The situation is complicated when the wall thickness t of hollow spheres is constant, and the diameter D changes. In order to more vividly describe the stress conditions of small and large spheres, we established a two-dimensional plane stress diagram, as shown in Fig. 7. The three-dimensional hollow hemisphere is simplified into a two-dimensional semicircle arc for analysis. O_1 and O_2 are, respectively, the spherical centres of small- and large-sized spheres, r_1 and r_2 are the radii of the two spheres, and P_1 and P_2 are, respectively, the vertices of the small and large sphere semicircles. Then, the force passing through the ver-

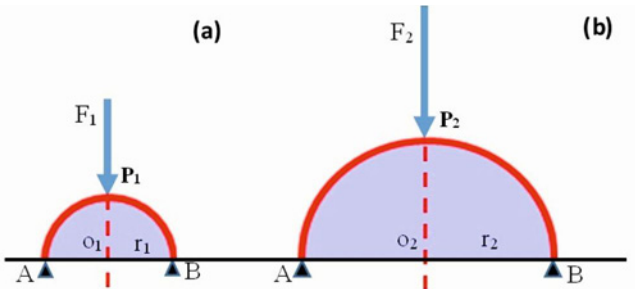

Fig. 7. Two-dimensional plane stress diagram of a small sphere and large sphere based on lever principle: (a) small sphere and (b) large sphere.

tices P_1 and P_2 and perpendicular to the straight line O_1O_2 is most likely to damage the spherical shell. According to the lever principle, for small particles, the torque (M_1) of point A and point B is equal, that is, $M_1 = F_1 \times r_1$; similarly, for large particles, the torque of point A and point B $M_2 = F_2 \times r_2$. When F_1 and F_2 are equal, since $r_2 > r_1$, $M_2 > M_1$, large particles are subject to greater torque and are more vulnerable to damage, or large hollow spheres can withstand less pressure. Large lever torque is the fundamental reason for the low compressive property of the syntactic foam prepared by large-diameter hollow spheres. M. Iser [54] showed that the larger the relative thickness of hollow microbeads, the higher their strength and the better the mechanical properties of syntactic foam materials. With the same thickness, the strength of hollow microbeads decreases with the increase of particle size, which affects the energy absorption capacity. M. Teherishargh [21] et al. have shown that the syntactic foam made by expanded perlite and A356 aluminium alloy has a similar conclusion. The smaller diameter and aperture have average distribution, good mechanical properties, even plastic deformation in compression, and obtain very high and stable plateau strength.

The syntactic foams with hollow spheres of 0.5–1 mm diameter were selected for different heat treatments. It can be seen from Fig. 6b and Table 5 that the syntactic foam's compression curves are obviously smooth after heat treatment, and the compression performance is greatly improved compared with the as-cast syntactic foam. The average compressive strength is 109.18 MPa, the average plateau strength is 81.61 MPa, the average energy absorption capacity is 50.84 MJ m^{-3}, and the average specific energy absorption is 28.64 kJ kg^{-1}, which is 24.07, 22.63, 37.04, and 40.53 % higher than for the as-cast state, respectively.

It can be seen from the microstructure of the syntactic foam after heat treatment in Fig. 5 that the most significant change in the microstructure of different heat treatments is the size of the Si phase. From

Table 7. Comparison of compressive energy absorption property of syntactic foams of the present work with some Al-matrix syntactic foams reported in recent years

Synthesis method	Matrix alloy	W (MJ m^{-3})	E_s (kJ kg^{-1})	Ref.	Year
Gravity infiltration	Al-Si-Cu-Mg alloy	56.33	30.45	Present work	2022
Powder metallurgy	1100 aluminium	48.74	22.15	[55]	2022
Stirring casting	Al-Mg alloy	146.88	57.38	[56]	2022
IFM	AFS	57.68	–	[57]	2021
Gravity infiltration	7055 Al alloy	48.14	28.04	[58]	2020
Stirring casting	TiC-TiB_2 reinforced Al alloy	7.5	–	[59]	2020
Gravity infiltration	6061 Al alloy	48.92	31.36	[60]	2019
Stirring casting	AA2014	65	32.66	[61]	2019
Gravity infiltration	ZL111 Al alloy	47.3	23.1	[62]	2019
Pressure infiltration	5A03 Al alloy	51.2	41.9	[2]	2018
Counter-gravity infiltration	A356 Al alloy	19.8	18.7	[19]	2018
Pressure infiltration	A356 Al alloy	6.6	8.7	[15]	2017
Pressure infiltration	5A06 Al alloy	62.8	44.9	[4]	2017
Stirring casting	AA2014 alloy	23.5	11.2	[63]	2017
Vacuum casting	Al-12Si alloy	7	6.2	[64]	2016
Pressure infiltration	A356 Al alloy	55.2	23.8	[65]	2016
Pressure infiltration	A356Al alloy	26.5	24.8	[22]	2015
Pressure infiltration	A356	13.9	13.4	[66]	2014
Pressure infiltration	A380 Al alloy	57.7	31	[67]	2014
Gravity infiltration	A355.0 Al alloy	18	15	[68]	2014
Pressure infiltration	A206 Al alloy	63.2	32.8	[13]	2013
Pressure infiltration	6082 Al alloy	30.9	25	[51]	2009

the point of view of the compression properties of syntactic foams with different heat treatments, the difference between their compression plateau height and specific energy absorption is tiny. The maximum difference of specific energy absorption is only about 2 kJ kg^{-1}, indicating that the change of microstructure caused by heat treatment has little effect on the energy absorption properties. We believe that the remarkable improvement of compression energy absorption performance after heat treatment is mainly attributed to the release of residual stress.

We know that the thermal expansion coefficient of alumina ceramics (6.8–7.8 $\times$ 10^{-6} K) is much smaller than that of metal aluminium (23.2 $\times$ 10^{-6} K). The solidification and cooling shrinkage of the aluminium alloy matrix are relatively large during the cooling process. In contrast, the cooling shrinkage of the aluminium oxide hollow sphere is minor, resulting in the aluminium alloy matrix's residual compressive stress around the hollow sphere's shell. This residual compressive stress harms the compression performance of syntactic foam and will reduce the compression performance. After homogenization heat treatment, the composition segregation and residual compressive stress of the matrix alloy are eliminated, so the compression energy absorption performance of the syntactic foam is greatly improved. Due to the coarsening of the Si phase after heat treatment, the strength of the matrix alloy is also damaged, and finally, the compressive strength and compression plateau height of the syntactic foam is reduced. As the morphology of Si in the sample normalized for 1 h keeps a small size, it has the best compression energy absorption performance. In contrast, the normalized + aged sample with Si becoming significantly coarse has lower compression performance.

In this paper, the aluminium matrix syntactic foam prepared by gravity infiltration technology has good compression energy absorption properties after heat treatment, with the highest specific energy absorption reaching 30.45 kJ kg^{-1}. Table 7 compares the best compression energy absorption performance of the syntactic foam prepared in this paper and some Al-matrix syntactic foam reported in recent years. It can be seen that the compression energy absorption performance obtained in this paper is superior to many reported Al-matrix syntactic foams. This result indicates that the Al-matrix syntactic foams prepared by a low-cost gravity infiltration and small Al_2O_3 hollow spheres have good engineering application potential.

4. Conclusions

Al-matrix syntactic foam filled with different Al_2O_{3-HS} sizes was successfully prepared by gravity infiltration process. The influence of hollow sphere size on the structure, quasi-static compression energy absorption of the as-cast syntactic foam, and the influ-

ence of homogenization and homogenization + ageing heat treatment on syntactic foam's compression energy absorption performance was studied. The following conclusions are drawn:

1. The Al_2O_{3-HS} is uniformly dispersed in the prepared Al-matrix syntactic foam, and fewer hollow spheres are filled with the matrix. The interface between the hollow spheres and the matrix is smooth, dense, and well-bonded. The density of the syntactic foam decreases with the increase of the hollow sphere size, and the maximum porosity reaches 42.75 %. The influence of the hollow sphere size on the microstructure of the syntactic foam matrix is not apparent, and the phase type and morphology of the matrix are not changed.

2. The diameter of hollow spheres significantly affects the compressive properties of syntactic foam. The average plateau strength and specific energy absorption of the syntactic foam increase with the decrease in hollow sphere size and the increase in the wall thickness ratio to diameter (t/D). The plateau strength and specific energy absorption of syntactic foam with hollow spheres of 0.5–1 mm diameter are the highest, reaching 66.55 MPa and 20.38 kJ kg^{-1}, respectively. The fundamental reason is that the small spheres in the syntactic foam are subject to less leverage torque and are not accessible to damage; they can withstand greater compressive stress.

3. After heat treatment, the syntactic foam's compression and energy absorption properties are significantly improved compared with the as-cast foam. The highest plateau strength, energy absorption capacity, and specific energy absorption occurred in the sample normalized for 1 h, reaching 87.71 MPa, 56.33 MJ m$^{-3,}$ and 30.45 kJ kg^{-1}, respectively. The improvement in the compressive properties of the heat-treated syntactic foam is mainly attributed to residual compressive stress release and compositional homogenization. The slight difference in the compressive properties among the heat-treated syntactic foams is mainly attributed to the change in the size of Si in the matrix.

Acknowledgements

The authors acknowledge the Special project of material processing of Guangxi Key Laboratory of Processing for Non-ferrous Metal and Featured Materials (2021GXMPSF04); Youth Fund of Guangxi Key Laboratory of Processing for Non-ferrous Metal and Featured Materials (GXYSYF1806); Special funds for local scientific and technological development under the guidance of the central government in 2021(GuiKeZY21195030); Guangxi Science and Technology Base and Talent Project in 2022 (GuiKeAD21238010).

References

[1] Y. Lin, Q. Zhang, J. Chang, H. Wang, X. Feng, J. Wang, Microstructural characterization and compression mechanical response of glass hollow spheres/Al syntactic foams with different Mg additions, Materials Science and Engineering A 766 (2019) 138338. https://doi.org/10.1016/j.msea.2019.138338

[2] Q. Zhang, Y. Lin, H. Chi, J. Chang, G. Wu, Quasi-static and dynamic compression behavior of glass cenospheres/5A03 syntactic foam and its sandwich structure, Composite Structures 183 (2018) 499–509. https://doi.org/https://doi.org/10.1016/j.compstruct.2017.05.024

[3] S. Broxtermann, M. Vesenjak, L. Krstulović-Opara, T. Fiedler, Quasi static and dynamic compression of zinc syntactic foams, Journal of Alloys and Compounds 768 (2018) 962–969. https://doi.org/https://doi.org/10.1016/j.jallcom.2018.07.215

[4] Y. Lin, Q. Zhang, F. Zhang, J. Chang, G. Wu, Microstructure and strength correlation of pure Al and Al-Mg syntactic foam composites subject to uniaxial compression, Materials Science and Engineering A 696 (2017) 236–247. https://doi.org/10.1016/j.msea.2017.04.060

[5] A. A. Chernousov, B. Y. B. Chan, Moderated nitridation of Al nanoflakes into open-pore composites for battery enclosures with improved crash and fire resistances, Journal of Alloys and Compounds 859 (2021) 157887. https://doi.org/10.1016/j.jallcom.2020.157887

[6] A. A. Chernousov, B. Y. B. Chan, Optimising in-situ nitridation in piled aluminium flakes for novel closed cell composites with high fracture stress and toughness, Materials & Design 150 (2018) 113–123. https://doi.org/10.1016/j.matdes.2018.04.020

[7] B. Katona, A. Szlancsik, T. Tábi, I. N. Orbulov, Compressive characteristics and low frequency damping of aluminium matrix syntactic foams, Materials Science and Engineering A 739 (2019) 140–148. https://doi.org/10.1016/j.msea.2018.10.014

[8] A. Szlancsik, B. Katona, D. Karoly, I. N. Orbulov, Notch (in)sensitivity of aluminum matrix syntactic foams, Materials (Basel) 12 (2019) 574. https://doi.org/10.3390/ma12040574

[9] A. Szlancsik, B. Katona, I. N. Orbulov, M. Taherishargh, T. Fiedler, Fatigue properties of EP/A356 aluminium matrix syntactic foams with different densities, IOP Conference Series: Materials Science and Engineering 426 (2018) 012045. https://doi.org/10.1088/1757-899x/426/1/012045

[10] G. Anbuchezhiyan, T. Muthuramalingam, B. Mohan, Effect of process parameters on mechanical properties of hollow glass microsphere reinforced magnesium alloy syntactic foams under vacuum die casting, Archives of Civil and Mechanical Engineering 18 (2018) 1645–1650. https://doi.org/https://doi.org/10.1016/j.acme.2018.07.008

[11] S. B. Başẗurk, M. Tanoğlu, Development and mechanical behavior of FML/aluminium foam sandwiches, Applied Composite Materials 20 (2012) 789–802. https://doi.org/10.1007/s10443-012-9306-3

[12] D. P. Mondal, N. Jha, A. Badkul, B. Gul, S. Rathod, S. Das, Effect of age hardening on compressive deformation behavior of Al-alloy (LM13) – cenosphere hybrid foam prepared using $CaCO_3$ as a foaming agent, Journal of Materials Research 28 (2013) 2528–2538. https://doi.org/10.1557/jmr.2013.197
[13] G. A. Rocha Rivero, B. F. Schultz, J. B. Ferguson, N. Gupta, P. K. Rohatgi, Compressive properties of Al-A206/SiC and Mg-AZ91/SiC syntactic foams, Journal of Materials Research 28 (2013) 2426–2435. https://doi.org/10.1557/jmr.2013.176
[14] Z. Chen, Y. Zhang, J. Wang, H. GangaRao, R. Liang, Y. Zhang, D. Hui, Experimental and modeling investigations of the behaviors of syntactic foam sandwich panels with lattice webs under crushing loads, Reviews on Advanced Materials Science 60 (2021) 450–465. https://doi.org/10.1515/rams-2021-0040
[15] S. Broxtermann, M. Taherishargh, I. V. Belova, G. E. Murch, T. Fiedler, On the compressive behaviour of high porosity expanded Perlite-Metal Syntactic Foam (P-MSF), Journal of Alloys and Compounds 691 (2017) 690–697. https://doi.org/10.1016/j.jallcom.2016.08.284
[16] Y. Lin, Q. Zhang, X. Ma, G. Wu, Mechanical behavior of pure Al and Al-Mg syntactic foam composites containing glass cenospheres, Composites Part A: Applied Science and Manufacturing 87 (2016) 194–202. https://doi.org/10.1016/j.compositesa.2016.05.001
[17] M. Su, H. Wang, H. Hao, Axial and radial compressive properties of alumina-aluminum matrix syntactic foam filled thin-walled tubes, Composite Structures 226 (2019) 111197. https://doi.org/10.1016/j.compstruct.2019.111197
[18] J. A. Santa Maria, B. F. Schultz, J. B. Ferguson, N. Gupta, P. K. Rohatgi, Effect of hollow sphere size and size distribution on the quasi-static and high strain rate compressive properties of Al-A380–Al_2O_3 syntactic foams, Journal of Materials Science 49 (2013) 1267–1278. https://doi.org/10.1007/s10853-013-7810-y
[19] M. Taherishargh, E. Linul, S. Broxtermann, T Fiedler, The mechanical properties of expanded perlite-aluminium syntactic foam at elevated temperatures, Journal of Alloys and Compounds 737 (2018) 590–596. https://doi.org/10.1016/j.jallcom.2017.12.083
[20] K. Al-Sahlani, S. Broxtermann, D. Lell, T. Fiedler, Effects of particle size on the microstructure and mechanical properties of expanded glass-metal syntactic foams, Materials Science and Engineering A 728 (2018) 80–87. https://doi.org/10.1016/j.msea.2018.04.103
[21] M. Taherishargh, M. A. Sulong, I. V. Belova, G. E. Murch, T. Fiedler, On the particle size effect in expanded perlite aluminium syntactic foam, Materials & Design 66 (2015) 294–303. https://doi.org/10.1016/j.matdes.2014.10.073
[22] M. Taherishargh, I. V. Belova, G. E. Murch, T. Fiedler, Pumice/aluminium syntactic foam, Materials Science and Engineering A 635 (2015) 102–108. https://doi.org/10.1016/j.msea.2015.03.061
[23] M. A. Sulong, M. Taherishargh, I. V. Belova, G. E. Murch, T. Fiedler, On the mechanical anisotropy of the compressive properties of aluminium perlite syntactic foam, Computational Materials Science 109 (2015) 258–265. https://doi.org/10.1016/j.commatsci.2015.07.038
[24] M. Garcia-Avila, A. Rabiei, Effect of sphere properties on microstructure and mechanical performance of cast composite metal foams, Metals 5 (2015) 822–835. https://doi.org/10.3390/met5020822
[25] T. Fiedler, I. V. Belova, G. E. Murch, On the thermal properties of expanded perlite – metallic syntactic foam, International Journal of Heat and Mass Transfer 90 (2015) 1009–1014. https://doi.org/10.1016/j.ijheatmasstransfer.2015.07.049
[26] M. Taherishargh, I. V. Belova, G. E. Murch, T. Fiedler, Low-density expanded perlite-aluminium syntactic foam, Materials Science and Engineering A 604 (2014) 127–134. https://doi.org/10.1016/j.msea.2014.03.003
[27] Y. Lin, Q. Zhang, T. Liu, H. Wang, J. Lu, Y. Ye, J. Wang, K. Zheng, Sol-gel MgO coating on glass microspheres for inhibiting excessive interfacial reaction in Al-Mg matrix syntactic foam, Journal of Alloys and Compounds 798 (2019) 59–66. https://doi.org/10.1016/j.jallcom.2019.05.258
[28] Z. Fan, Y. Miao, Z. Wang, B. Zhang, H. Ma, Effect of the cenospheres size and internally lateral constraints on dynamic compressive behavior of fly ash cenospheres polyurethane syntactic foams, Composites Part B 171 (2019) 329–338. https://doi.org/10.1016/j.compositesb.2019.05.008
[29] I. N. Orbulov, A. Kemény, Á. Filep, Z. Gácsi, Compressive characteristics of bimodal aluminium matrix syntactic foams, Composites Part A: Applied Science and Manufacturing 124 (2019) 105479. https://doi.org/10.1016/j.compositesa.2019.105479
[30] H. Puga, V. H. Carneiro, C. Jesus, J. Pereira, V. Lopes, Influence of particle diameter in mechanical performance of Al expanded clay syntactic foams, Composite Structures 184 (2018) 698–703. https://doi.org/10.1016/j.compstruct.2017.10.040
[31] C. A. Vogiatzis, S. M. Skolianos, On the sintering mechanisms and microstructure of aluminium-ceramic cenospheres syntactic foams produced by powder metallurgy route, Composites Part A: Applied Science and Manufacturing 82 (2016) 8–19. https://doi.org/10.1016/j.compositesa.2015.11.037
[32] C. A. Vogiatzis, A. Tsouknidas, D. T. Kountouras, S. Skolianos, Aluminum–ceramic cenospheres syntactic foams produced by powder metallurgy route, Materials & Design 85 (2015) 444–454. https://doi.org/10.1016/j.matdes.2015.06.154
[33] A. Szlancsik, B. Katona, A. Kemeny, D. Karoly, On the filler materials of metal matrix syntactic foams, Materials (Basel) 12 (2019) 2023. https://doi.org/10.3390/ma12122023
[34] A. Kemény, B. Leveles, T. Bubonyi, I. N. Orbulov, Effect of particle size and volume ratio of ceramic hollow spheres on the mechanical properties of bimodal composite metal foams, Composites Part A: Applied Science and Manufacturing 140 (2021) 106152. https://doi.org/10.1016/j.compositesa.2020.106152
[35] J. Grilo, V. H. Carneiro, J. C. Teixeira, H. Puga, Manufacturing methodology on casting-based aluminium matrix composites: Systematic review, Metals 11 (2021) 436. https://doi.org/10.3390/met11030436
[36] I. N. Orbulov, A. Szlancsik, A. Kemény, D. Kincses, Compressive mechanical properties of low-cost, aluminium matrix syntactic foams, Composites Part A: Applied Science and Manufacturing 135 (2020)

105923.
https://doi.org/10.1016/j.compositesa.2020.105923
[37] A. Szlancsik, B. Katona, K. Bobor, K. Májlinger, I. N. Orbulov, Compressive behaviour of aluminium matrix syntactic foams reinforced by iron hollow spheres, Materials & Design 83 (2015) 230–237. https://doi.org/10.1016/j.matdes.2015.06.011
[38] A Bahrami, M. I. Pech-Canul, C. A. Gutiérrez, N. Soltani, Wetting and reaction characteristics of crystalline and amorphous SiO_2 derived rice-husk ash and SiO_2/SiC substrates with Al-Si-Mg alloys, Applied Surface Science 357 (2015) 1104–1113. https://doi.org/10.1016/j.apsusc.2015.09.137
[39] G. Castro, S. R. Nutt, Synthesis of syntactic steel foam using gravity-fed infiltration, Materials Science and Engineering A 553 (2012) 89–95. https://doi.org/10.1016/j.msea.2012.05.097
[40] L. Pan, Y. Yang, M. U. Ahsan, D. D. Luong, N. Gupta, A. Kumar, P. K. Rohatgi, Zn-matrix syntactic foams: Effect of heat treatment on microstructure and compressive properties, Science and Engineering A 731 (2018) 413–422. https://doi.org/10.1016/j.msea.2018.06.072
[41] G. Anbuchezhiyan, B. Mohan, D. Sathianarayanan, T. Muthuramalingam, Synthesis and characterization of hollow glass microspheres reinforced magnesium alloy matrix syntactic foam, Journal of Alloys and Compounds 719 (2017) 125–132. https://doi.org/10.1016/j.jallcom.2017.05.153
[42] D. D. Luong, V. C. Shunmugasamy, N. Gupta, D. Lehmhus, J. Weise, J. Baumeister, Quasi-static and high strain rates compressive response of iron and Invar matrix syntactic foams, Materials & Design 66 (2015) 516–531. https://doi.org/10.1016/j.matdes.2014.07.030
[43] Y. Lin, Q. Zhang, F. Zhang, J. Chang, G. Wu, Microstructure and strength correlation of pure Al and Al-Mg syntactic foam composites subject to uniaxial compression, Materials Science and Engineering A 696 (2017) 236–247. https://doi.org/10.1016/j.msea.2017.04.060
[44] L. Pan, Y. Yang, M. U. Ahsan, D. D. Luong, N. Gupta, A. Kumar, P. K. Rohatgi, Zn-matrix syntactic foams: Effect of heat treatment on microstructure and compressive properties, Materials Science and Engineering A 731 (2018) 413–422. https://doi.org/10.1016/j.msea.2018.06.072
[45] A. Daoud, Compressive response and energy absorption of foamed A359–Al_2O_3 particle composites, Journal of Alloys and Compounds 486 (2009) 597–605. https://doi.org/10.1016/j.jallcom.2009.07.013
[46] J. A. Liu, S. R. Yu, Z. Q. Hu, Y. H. Liu, X. Y. Zhu, Deformation and energy absorption characteristic of Al_2O_{3f}/Zn-Al composite foams during compression, Journal of Alloys and Compounds 506 (2010) 620–625. https://doi.org/10.1016/j.jallcom.2010.06.107
[47] X. Dong, S. Amirkhanlou, S. Ji, Formation of strength platform in cast Al-Si-Mg-Cu alloys, Scientific Reports 9 (2019) 9582. https://doi.org/10.1038/s41598-019-46134-7
[48] V. Raghavan, Al-Si-Ti (Aluminum-Silicon-Titanium), Journal of Phase Equilibria and Diffusion 30 (2008) 82–83. https://doi.org/10.1007/s11669-008-9435-4
[49] Y. Lin, Q. Zhang, G. Wu, Interfacial microstructure and compressive properties of Al-Mg syntactic foam reinforced with glass cenospheres, Journal of Alloys and Compounds 655 (2016) 301–308. https://doi.org/10.1016/j.jallcom.2015.09.175
[50] B. Soni, S. Biswas, Mass-scale processing of open-cell metallic foams by pressurized casting method, Journal of Porous Materials 24 (2016) 29–37. https://doi.org/10.1007/s10934-016-0233-9
[51] X. F. Tao, L. P. Zhang, Y. Y. Zhao, Al matrix syntactic foam fabricated with bimodal ceramic microspheres, Materials & Design 60 (2009) 2732–2736. https://doi.org/10.1016/j.matdes.2008.11.005
[52] G. H. Wu, Z. Y. Dou, D. L. Sun, L. T. Jiang, B. S. Ding, B. F. He, Compression behaviors of cenosphere-pure aluminum syntactic foams, Scripta Materialia 56 (2007) 221–224. https://doi.org/10.1016/j.scriptamat.2006.10.008
[53] M. Taherishargh, I. V. Belova, G. E. Murch, T. Fiedler, Low-density expanded perlite–aluminium syntactic foam, Materials Science and Engineering A 604 (2014) 127–134. https://doi.org/10.1016/j.msea.2014.03.003
[54] M. Kiser, M. Y. He, F. W. Zok, The mechanical response of ceramic microballoon reinforced aluminum matrix composites under compressive loading, Acta Materialia 47 (1999) 2685–2694. https://doi.org/10.1016/S1359-6454(99)00129-9
[55] M. Cao, F. Jian, C. Guo, Y. Li, T. Yu, R. Qin, Interface characterization and mechanical property of an aluminum matrix syntactic foam with multi-shelled hollow sphere structure, Ceramics International 48 (2022) 18821–1883. https://doi.org/10.1016/j.ceramint.2022.03.159
[56] J. Jung, S.-H. Kim, J.-H. Kang, J. Park, W.-K. Kim, C.-Y. Lim, Y.-H. Park, Compressive strength modeling and validation of cenosphere-reinforced aluminum–magnesium-matrix-based syntactic foams, Materials Science and Engineering A 849 (2022) 143452. https://doi.org/10.1016/j.msea.2022.143452
[57] Z. Zhang, H. Feng, T. Xu, W. Xin, J. Ding, N. Liu, Z. Wang, Y. Wang, X. Xia, Y. Liu, Compression performances of integral-forming aluminum foam sandwich, Composite Structures 283 (2022) 115090. https://doi.org/10.1016/j.compstruct.2021.115090
[58] D. W. Rao, Y. W. Yang, Y. Huang, J. B. Sun, L. W. Pan, Z. L. Hu, Microstructure and compressive properties of aluminum matrix syntactic foams containing Al_2O_3 hollow particles, Kovove Mater. 58 (2020) 395–407. https://doi.org/10.4149/km_2020_6_395
[59] X. An, Y. Liu, J. Ye, X. Li, Fabrication of in-situ TiC–TiB_2 reinforced Al foam with enhanced properties, Journal of Alloys and Compounds 825 (2020) 153969. https://doi.org/10.1016/j.jallcom.2020.153969
[60] L. Pan, D. Rao, Y. Yang, J. Qiu, J. Sun, N. Gupta, Z. Hu, Gravity casting of aluminum-Al_2O_3 hollow sphere syntactic foams for improved compressive properties, Journal of Porous Materials 27 (2020) 1127–1137. https://doi.org/10.1007/s10934-020-00889-x
[61] S. Sahu, M. Z. Ansari, D. P. Mondal, C. Cho, Quasi-static compressive behaviour of aluminium cenosphere syntactic foams, Materials Science and Technology 35 (2019) 856–864. https://doi.org/10.1080/02670836.2019.1593670

[62] M. Su, H. Wang, H. Hao, Axial and radial compressive properties of alumina-aluminum matrix syntactic foam filled thin-walled tubes, Composite Structures 226 (2019) 111197. https://doi.org/10.1016/j.compstruct.2019.111197

[63] S. Birla, D. P. Mondal, S. Das, N. Prasanth, A. K. Jha, A. N. C. Venkat, Compressive deformation behavior of highly porous AA2014-cenosphere closed cell hybrid foam prepared using CaH_2 as foaming agent: Comparison with aluminum foam and syntactic foam, Transactions of the Indian Institute of Metals 70 (2017) 1827–1840. https://doi.org/10.1007/s12666-016-0984-7

[64] A. Wright, A Kennedy, The processing and properties of syntactic Al foams containing low cost expanded glass particles, Advanced Engineering Materials 19 (2017) 1600467. https://doi.org/10.1002/adem.201600467

[65] M. Taherishargh, M. Vesenjak, I. V. Belova, L. Krstulović-Opara, G. E. Murch, T. Fiedler, In situ manufacturing and mechanical properties of syntactic foam filled tubes, Materials & Design 99 (2016) 356–368. https://doi.org/10.1016/j.matdes.2016.03.077

[66] T. Fiedler, M. Taherishargh, L. Krstulović-Opara, M. Vesenjak, Dynamic compressive loading of expanded perlite/aluminum syntactic foam, Materials Science and Engineering A 626 (2015) 296–304. https://doi.org/https://doi.org/10.1016/j.msea.2014.12.032

[67] J. A. Santa Maria, B. F. Schultz, J. B. Ferguson, N. Gupta, P. K. Rohatgi, Effect of hollow sphere size and size distribution on the quasi-static and high strain rate compressive properties of Al-A380–Al_2O_3 syntactic foams, Journal of Materials Science 49 (2014) 1267–1278. https://doi.org/10.1007/s10853-013-7810-y

[68] S. Bazzaz Bonabi, J. Kahani Khabushan, R. Kahani, A. Honarbakhsh Raouf, Fabrication of metallic composite foam using ceramic porous spheres "Light expanded clay aggregate" via casting process, Materials & Design 64 (2014) 310–315. https://doi.org/10.1016/j.matdes.2014.07.061